



A reliability-based design concept for lithium-ion battery pack in electric vehicles



Zhitao Liu^a, CherMing Tan^{a,b,c,*}, Feng Leng^{a,b}

^a TUM CREATE, 1 CREATE Way, #10-02 CREATE Tower, Singapore 138602, Singapore

^b School of Electrical and Electronic Engineering, Nanyang Technological University, Nanyang Avenue, Singapore 639798, Singapore

^c Chang Gung University, Department of Electronics Engineering, 259 Wen-Hwa 1st Road, Kwei-Shan, Tao-Yuan 333, Taiwan, ROC

ARTICLE INFO

Article history:

Received 28 October 2013

Received in revised form

3 September 2014

Accepted 7 October 2014

Available online 29 October 2014

Keywords:

Multi-state systems

Reliability

Universal generating function

State of health

Battery pack

Electric vehicle

ABSTRACT

Battery technology is an enabling technology for electric vehicles (EVs), and improving its safety and reliability while reducing its cost will benefit its application to EVs. In this paper, a method on the design and analysis of lithium-ion (Li-ion) battery pack from the reliability perspective is presented. The analysis is based on the degradation of the battery pack, which is related to the cells configuration in the battery pack and the state of health (SoH) of all the Li-ion cells in the pack. Universal Generating Function (UGF) technique is used for reliability analysis. As adding new battery cells to the battery pack in the production process can improve its reliability but it also increases cost, tradeoff between the number of the redundant battery cells, the configuration of the redundant cells and their reliability is investigated in this work.

© 2014 Elsevier Ltd. All rights reserved.

1. Introduction

In view of the fossil fuel depletion and the emission of greenhouse gases (GHG) with the fossil fuel, and the fact that transportation is a major source of GHG emission and usage of the fossil fuel, research and development of electric vehicles (EVs) are blooming significantly. With EVs, their energy sources can be renewable clean energy sources through the recharging of Li-ion battery packs from these clean energy sources, and no GHG emission occurs with EVs.

These EVs are driven by electric motors instead of internal combustion engines. These motors are powered by the Li-ion battery packs in the vehicles. Li-ion batteries are used because they have the highest energy and power densities, and their life time is sufficiently longer [1]. In fact, it is because of the Li-ion battery technology that enables EVs to be a realistic product that we see in the market today worldwide [2].

While EVs are now commercial products, there are three main challenges that are being researched into, namely the limited driving range, long batteries charging time and high cost of the battery pack [2]. All these challenges are closely link to the

applications of the Li-ion battery pack in EVs. The high cost of the pack in turn is related to the reliability of the pack because if the pack has low charge/discharge cycle life time, the replacement frequency of the pack will be high, and this will increase the operating cost of the EVs.

Currently, the battery pack of EV contains more than 100 Li-ion cells, and when one cell becomes aged, other cells will have to carry the load and this can cause other cells to degrade rapidly. On the other hand, due to the safety consideration, one cannot open the pack and replace the aged cells in the pack. Thus, when a few cells get aged, the entire pack will have to be replaced and sent to the workshop, and this increases the operating cost of EVs significantly and unnecessary.

The above-mentioned situations will happen even with the use of reliable cells, and thus to reduce the unnecessary replacement of the pack and to prolong the life span of the pack, redundant cells are designed in the pack [3].

Several works reported the reliability analysis of battery packs, and they can be divided into the following categories of focus. The references quoted below are the typical papers selected for each category.

1.1. Thermal management of battery pack to improve pack reliability

The temperature in battery pack is an important factor which affects the safety and reliability of the cells when the vehicle is

* Corresponding author at: TUM CREATE, 1 CREATE Way, #10-02 CREATE Tower, Singapore 138602, Singapore.

E-mail addresses: zhitao.liu@tum-create.edu.sg (Z. Liu), cmtan@mail.cgu.edu.tw (C. Tan), fleng001@e.ntu.edu.sg (F. Leng).

running. Using thermal management in BMS (battery management system) can improve the reliability of the battery pack. In this category of research works, the heat generation model, the methods of cooling and air flow in the battery packs are investigated [4–7].

1.2. Cell redundancy and configuration to improve pack reliability

In order to improve the reliability of the battery packs, different configurations of cells and the use of cell redundancy, coupled with appropriate designs of DC/DC converters are proposed [8–10]. However, no quantitative relationship between the pack reliability and redundant cells configuration is discussed.

1.3. Prognostic and health management for battery packs

Since there are inevitable differences in the cells, a cell in battery packs could become overcharged and/or over-discharged. This could in turn reduce the lifetime of the packs. Generally speaking, the health state of an individual degraded cell is difficult to detect in a battery pack. To ensure safe driving, the battery packs are routinely replaced even though they do not exhibit any problems, but this will increase the maintenance cost for the drivers. Prognostic and health monitoring (PHM) technology is thus proposed to monitor the battery pack in the EVs. It can monitor the battery pack states during their operations, and extend their useful lives correspondingly [11].

In order to improve the reliability and safety of a battery pack, one simple and direct method is to add redundant cells to the battery pack, but two associated questions should be investigated. First, the configuration of the redundant cells in the battery pack; Second, the number of redundant cells for cost effectiveness. In this work, a design concept is developed to answer these two questions quantitatively.

For the first question, the effect of cells configuration in the pack on the pack’s reliability is generally overlooked. However, the effect can be significant. Let us illustrate the effect with the following idealistic example.

Assuming perfect conversion such that the total power in the battery pack can be converted into the required voltages and currents at a given output power without any loss, Figs. 1–3 show four possible configurations of 10 identical cells in a battery pack.

Assuming every cell has two states, namely the normal and abnormal, and the probability of a cell in the abnormal state is x . Given that the different battery packs are to supply the same power P , the current I through each cell in the 4 different configurations will be the same and equal to $I = (P/10V_0)$, where V_0 is the voltage of a cell. If we assume that the battery packs are charged/discharged for the same number of cycles, and the degradation of the cells are identical, the probability of normal state for the battery packs with different configurations could be calculated as follows, and they are shown in Fig. 4.

$$P_a = 1 - [1 - (1 - x)^5]^2 \tag{1a}$$

$$P_b = (1 - x^2)^5 \tag{1b}$$

$$P_c = 1 - [1 - (1 - x)^2]^5 \tag{1c}$$

$$P_d = (1 - x^5)^2 \tag{1d}$$

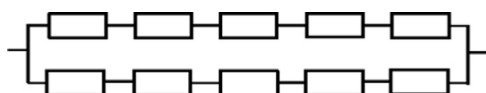


Fig. 1. Structure a.

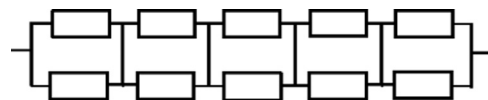


Fig. 2. Structure b.

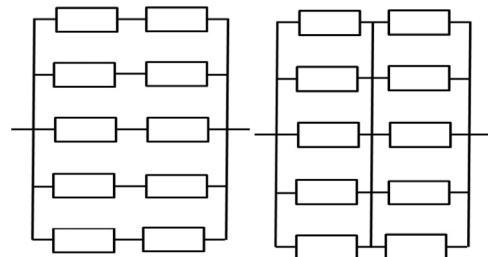


Fig. 3. Structure c (left) and structure d (right).

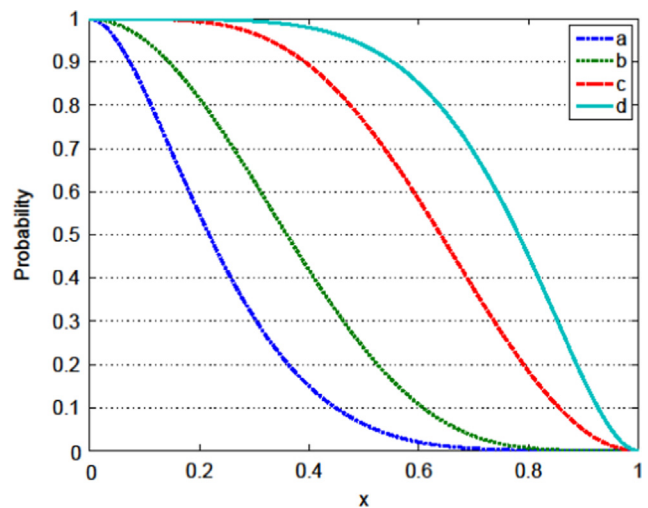


Fig. 4. The probability for different structures.

From the above example, we can see that the reliabilities of the parallel-series structures, i.e. structures b and d are higher than the series-parallel configurations, i.e. structure a and c, with structure d being the best for the reliability. Therefore, if the redundant cell number and cost are not in consideration, adding more parallel branches in battery pack will be preferred, and its reliability can be greatly enhanced [12]. With cost consideration, tradeoff between reliability and the number of the cells is inevitable, and this is the focus of this work.

State of health (SoH) of the cells will be used here for analysis. SoH is defined as a variable which reflects the general health condition of a cell and its ability to deliver specified energy or charge as compared to its fresh state. The knowledge of SoH can be used to recognize ongoing or abrupt degradation of the cells and to prevent possible failure.

There have been many SoH methods in literatures [13–17], and none is considered as standard currently. To illustrate our design concept, any SoH method that models the effects of temperature, charge–discharge cycling and current on cell capacity fading, and its rate capability losses will be good enough for our purpose. In this work, we choose the model proposed in [17], which is also used by others [18,19]. This model is based on the electrochemistry mechanisms of the cells. With this model, a capacity fade prediction that describes the degradation effects from the charge and discharge cycling number, temperature and the discharge rate is possible.

To calculate the reliability of a battery pack using the cell’s SoH, multi-state systems (MSS) and universal generating function (UGF)

techniques are employed in this work. Many real-world systems are composed of multi-state components, which have different performance levels and failure modes with various effects on the system's entire performance. Such systems are called multi-state systems [20]. For MSS, the system performance will be essentially different for components with different performance rates. In order to calculate the reliability of MSS, universal generating function technique is applied.

The UGF methodology is an essential tool to obtain the performance distribution of an overall system from the performance distributions of the individual elements in the system. UGF has been used to analyze the reliability and optimize the structures of MSS [21,22], and it is found to be effective and can be applied to solve many problems of MSS. Tan et al. [23,24] applied UGF to study the reliability of a repairable system under the various maintenance schemes, and demonstrate the significant benefit of predictive maintenance. UGF was also used to analyze the reliability of primary battery packs with defined required capacities and voltages in [25].

There have been many reliability-based design methodologies for different applications. A scheme is proposed to define optimum design domains of LED-based luminaires for a given light output requirement by considering their reliability in [26]. Another method is proposed for reliability-based design optimization on the basis of the concept of reliable design space, within which all design could satisfy the reliability requirements in [27]. In [28], an integrated algorithm system is proposed to implement the reliability-based design for offshore towers that enable them to perform well in complicated environment conditions. A mixed redundancy strategy is proposed by Ardakan et al. [29] to determine the component type, redundancy level, number of active and cold-standby units for system in order to maximize the system reliability. Zhang et al. [30] provided a design for a modular converter system with consideration of the trade-offs between reliability, cost and space consumption, and they provided insights and guidance for designers in their decision-making. However, none of them using MSS and

UGF for the design assessment. As mentioned before, battery pack degradation is a complex multi-states process for each cell in the pack, and it depends on many factors, such as cell number, cell configuration, cycle number and state of health etc., hence MSS is needed for the modelling of the cells' reliability and UGF is required to combine the different states of the cells for the reliability evaluation of the entire pack. The above mentioned design methods are not applicable to battery pack for its design for reliability.

The usage of MSS and UGF combination have been used for the study of predictive maintenance which is reliability based [23,24]. Li et al. [31] used UGF to develop a MSS model for reliability assessment of a distributed systems. Tian et al. [32] applied UGF for a MSS series-parallel system to determine the optimal component reliabilities and redundancy levels for each sub-system. Their optimization objective was cost, and different versions of the components with different performance rates were also considered.

In contrast to the work of Tian et al. [32], we consider only one version of battery cells, but their performances and health states are varying and governed by a statistical distribution. Also, the reliability of a battery pack is sensitive to the cells connection configuration as illustrated earlier, and such configuration is considered in the design for reliability. Furthermore, the purpose of this work is to provide a design for a given required reliability of the battery pack with minimum cost, and thus reliability curve of a battery pack is needed. Thus the method of Tian et al. [32] cannot be applied directly, and a new methodology is proposed in this work.

Using the combination of MSS and UGF, we propose a reliability-based design concept for Lithium-ion battery packs, considering the tradeoff between the number of the redundant battery cells, the configuration of the redundant cells, and their reliability. This concept provides a solution for the battery pack designers.

According to the capacity fade model of Li-ion cells [17], we first calculate the SoH of the cells. By assuming the SoH of all the cells following normal distribution, UGF technique is applied to calculate the reliability of a battery pack. We will show the reliability change by adding redundant cells to the battery pack with different configurations, and the battery pack design with the highest reliability and minimum number of redundant cells.

The remaining paper is organized as follows. The capacity fade model of the Li-ion cells is given in Section 2, and the MSS for describing the SoH of a battery pack and the UGF technique for calculating its reliability are shown in Section 3. In Section 4, the reliability of a battery pack is first calculated based on the MSS and UGF techniques, and the effects from the cycling number, temperature and the discharge rate are simulated. The reliabilities of

Table 1
Values of the parameters in Eq. (6) at different temperatures [17].

Cycling temperature (°C)	k_1 [cycle ⁻²]	k_2 [cycle ⁻¹]	k_3 [A ⁻¹]
25	8.5×10^{-8}	2.5×10^{-4}	$2.68 \times 10^{-2} (\leq 300)$ $7.26 \times 10^{-2} (\leq 800)$
50	1.6×10^{-6}	2.9×10^{-4}	$5.20 \times 10^{-2} (\leq 300)$ $6.82 \times 10^{-2} (\leq 500)$

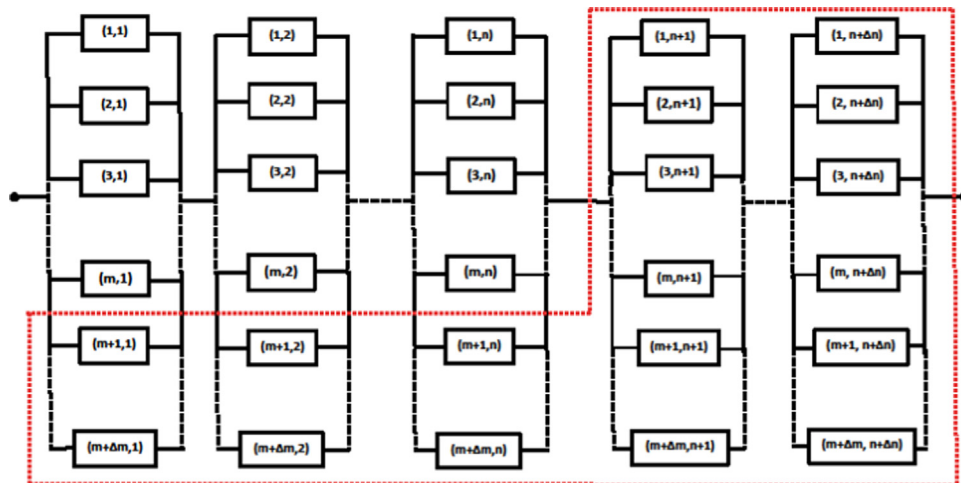


Fig. 5. The configuration of the battery pack with redundant cells. (For interpretation of the references to color in this figure legend, the reader is referred to the web version of this article.)

the battery pack by adding redundant cells with different structures at different temperatures are then calculated. Section 5 shows our experimental plan for the verification of our design concept and the associated challenges. Conclusions and future works are given in Section 6.

2. The capacity fade model of lithium-ion battery cell

The SoH of a lithium-ion battery cell is defined as [33,34],

$$\text{SoH} = \frac{Q_{\max}(\text{aged})}{Q_{\max}(\text{new})} \tag{2}$$

$$Q_{\max}(\text{aged}) = Q_{\max}(\text{new}) - Q_{\max}(\text{fade}) \tag{3}$$

where $Q_{\max}(\text{aged})$ and $Q_{\max}(\text{new})$ are the maximum amount of charge that can be drawn from the aged and new batteries, respectively. $Q_{\max}(\text{fade})$ represents the capacity faded due to temperature, cycle number and the discharge rate.

According to the analysis in [17], the faded capacity consists of three parts. The first part is the loss in capacity due to an increase in resistance at both electrodes. The second part is the loss of lithiation capacity at both electrodes. The third part is due to loss of active material Li^+ in the cell. These three parts of a cell are affected by the cell temperature, the number of its charging and discharging cycles and its discharging rate (also known as C-rate). A semi-empirical capacity fading model, which considers the effects of cell temperature and the number of charging/discharging cycles is given below [17]

$$Q_{\text{lost}}(T, N) = \text{SOC}_{\text{lost}} \times Q_{\max}(\text{new}) \tag{4a}$$

$$\frac{d\text{SOC}_{\text{lost}}}{dN} = k_1 N + k_2 \tag{4b}$$

where $Q_{\text{lost}}(T, N)$ represents the capacity fading due to the charge/discharge cycle number N and temperature. The parameter k_1 accounts for the capacity losses that increase rapidly during the conditions such as cycling at high temperature, and k_2 is a factor to account for capacity losses under the normal conditions of cycling. Due to the increase in film resistance during cycling, the rate capability of the cells decreases. However, Eq. (4) can only be used at very low discharge rates, and it is necessary to update the above model for the capacity fade by considering the C-rate. According to the experiment in [17], the discharge capacity loss is linear with respect to the C-rate,

$$Q_{\text{lost}}(i) = k_3 i \tag{5}$$

with the capacity analysis [17] and Eqs. (4) and (5), we therefore have $Q_{\max}(\text{fade}) = Q_{\text{lost}}(T, N) + Q_{\text{lost}}(i)$, and the SoH of a battery cell can be calculated as follows,

$$\text{SoH} = 1 - \left(\frac{1}{2} k_1 N^2 + k_2 N \right) - \frac{k_3}{Q_{\max}(\text{new})} i \tag{6}$$

where i is the discharge rate. The derivation of Eq. (6) is shown in Appendix A. The values of the coefficients in Eq. (6) are shown in Table 1, where “ ≤ 300 ” represents the cycle number of the cell is less than 300, and similarly for others.

3. Multi-state battery pack systems

Consider the configuration of a battery pack as shown in Fig. 5. The position of each cell in the battery pack is referenced by (i, j) , where $i = 1, 2, \dots, m, m+1, \dots, m+\Delta m$; $j = 1, 2, \dots, n, n+1, \dots, n+\Delta n$. The cells in the box enclosed by the red dashed lines are the redundant cells. For ease of discussion, the battery pack that contains $m \times n$ cells is denoted as battery pack I, and the battery pack with active

redundant cells added, i.e. having $(m+\Delta m) \times (n+\Delta n)$ cells, is denoted as battery pack II.

In order to calculate the reliability of the battery pack using the SoH of all the cells in the battery pack, the SoH is assumed to be a normal distribution $N(\mu, \sigma^2)$ at any instant of time. This means that Eq. (6) provides only the mean SoH of the cells in a battery pack, and the individual cell's SoH is different from each others due to material variations of the fresh cells, the different degree of damages and their susceptibility to these damages during the charge/discharge cycles and the cell balancing method in the battery management systems. As the number of cells is usually large in a battery pack (> 100), the cells' SoH in the battery pack can be considered as a

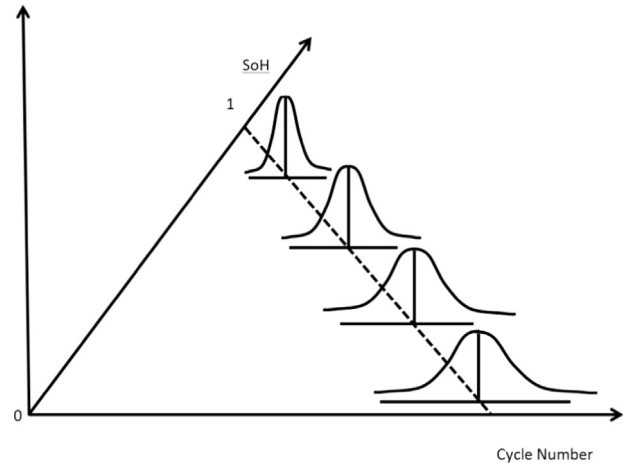


Fig. 6. The cell's SoH distribution in the battery pack.

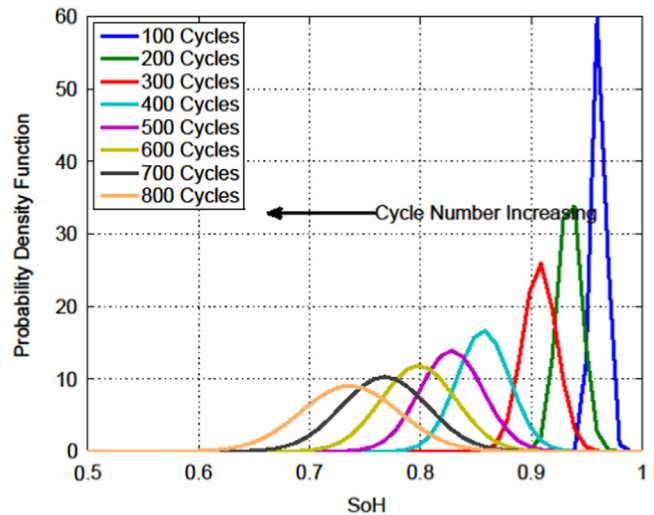


Fig. 7. The probability density function at 0.5 C rate and 25 °C.

Table 2
Probability for the cell's SoH levels at 0.5 C and 25 °C.

Cycle number	$\geq 90\%$	80–90%	70–80%	60–70%	$\leq 60\%$
100	1	0	0	0	0
200	0.9994	0.0006	0	0	0
300	0.6935	0.3065	0	0	0
400	0.0354	0.9561	0.0085	0	0
500	0.0060	0.8304	0.1636	0	0
600	0.0012	0.4798	0.5137	0.0017	0
700	0.0003	0.2028	0.7572	0.0397	0
800	0.0001	0.0740	0.7229	0.2020	0.0009

normal distribution, according to the central limit theorem. Explanation of the central limit theorem can be found in Appendix A.

For a given electric vehicle with $m \times n$ cells in a battery pack, assuming that the pack's energy capacity can supply the required power up to N charge/discharge cycle, then with the addition of $(m + \Delta m) \times (n + \Delta n) - m \times n$ redundant cells in the new battery pack, the maximum charge/discharge cycle N_{new} , which the new battery pack needs to supply the same required power, will be given as follows,

$$N_{new} = \frac{mnN}{(m + \Delta m)(n + \Delta n)} \quad (7)$$

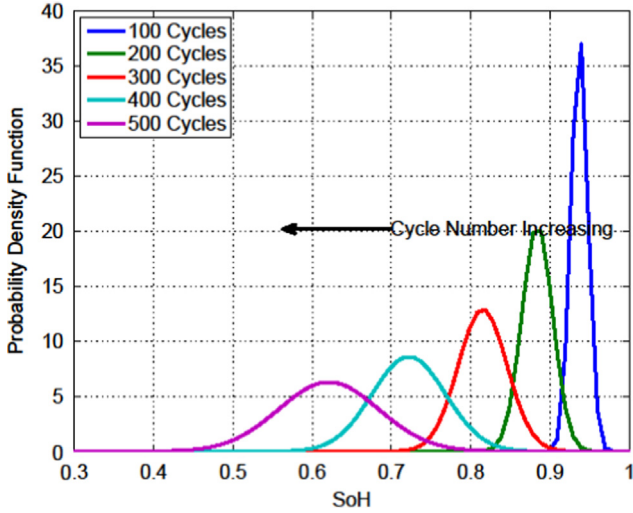


Fig. 8. The probability density function at 0.5 C rate and 50 °C.

Table 3
Probability for the cell's SoH levels at 0.5 C rate and 50 °C.

Cycle number	≥ 90%	80–90%	70–80%	60–70%	≤ 60%
100	0.9998	0.0002	0	0	0
200	0.2040	0.7960	0	0	0
300	0.0029	0.6838	0.3132	0.0001	0
400	0.0001	0.0459	0.6357	0.3140	0.0043
500	0	0.0023	0.1030	0.5243	0.3704

Table 4
The reliability $R(G_s \geq 80\%)$ of the battery pack at 25 °C.

Cycle number	0.5 C	1 C	1.5 C	2 C
100	1	1	1	1
200	1	1	1	1
300	1	1	1	1
400	0.9996	0.7330	0.0516	0.0004
500	0.8732	0.1139	0.0011	0
600	0.2082	0.0029	0	0
700	0.0065	0	0	0
800	0.0001	0	0	0

Table 5
The reliability $R(G_s \geq 80\%)$ of the battery pack at 50 °C.

Cycle number	0.5 C	1 C	1.5 C	2 C
100	1	1	1	0.9998
200	1	0.9997	0.9225	0.3667
300	0.5965	0.0860	0.0033	0.0001
400	0	0	0	0
500	0	0	0	0

As the EV needs the same power P for driving on the road regardless of battery pack I or II, the discharging rates of the cells for both battery packs are related as follows, if new Δm parallel branches are added to battery pack II,

$$i = \frac{m}{m + \Delta m} \times I \quad (8)$$

where I is the individual discharging current in the $m \times n$ battery pack I. Similarly, with new Δn series branches, the cell discharging rates' relationship is

$$i = \frac{n}{n + \Delta n} \times I \quad (9)$$

So if Δm parallel and Δn series branches are added to the battery pack, the discharging rate becomes

$$i = \frac{mn}{(m + \Delta m)(n + \Delta n)} \times I \quad (10)$$

3.1. Universal generating function

To apply UGF for the reliability computation of the battery pack, the cell's SoH degradation is divided into different levels so as to convert it into a MSS model. Each level is defined by a range of SoH values, such as 100–90%, 90–80%, etc. In other words, we categorize the SoH of every cell in the battery pack into $\geq 90\%$, 90–80%, 80–70%, 70–60% and $\leq 60\%$ levels, and the MSS model for a battery pack has 5 levels.

With reference to Fig. 5, we define $k_{(i,j)}$ ($= 4, 3, 2, 1, 0$) as the SoH level of the cell (i, j) in the battery pack, and $P_{(i,j)}(k_{(i,j)})$ as the probability of cell (i, j) at level $k_{(i,j)}$. Using the methodology of UGF [18], the u -function of the cell (i, j) is

$$u_{(i,j)}(z) = \sum P_{(i,j)}(k_{(i,j)}) z^{k_{(i,j)}} \quad (11)$$

and the UGF of the battery pack is

$$U(z) = \prod_{i=1}^m \prod_{j=1}^n u_{(i,j)}(z) \quad (12)$$

with the parallel-series structure of the battery pack, the performance G_s of the system takes the form [18],

$$G_s = \min_{j=1, \dots, n+\Delta n} \max_{i=1, \dots, m+\Delta m} g_{(i,j)}(k_{(i,j)}) \quad (13)$$

where $g_{(i,j)}(k_{(i,j)})$ represents the SoH of the cell (i, j) at level $k_{i,j}$. Let $\bar{s} = \inf\{s: G_s \geq W\}$, where W is the minimum user-set threshold demand value, the system can be divided into two disjoint subsets of acceptable states $\{\bar{s}, \bar{s} + 1, \dots, 4\}$ and unacceptable states $\{0, 1, \dots, \bar{s} - 1\}$. The reliability function R for a given user demand W can then be written as,

$$R = P(G_s \geq W) = \sum_{k=\bar{s}}^4 P(k) \quad (14)$$

where $P(k)$ is the state probability of the battery pack at k level.

Table 6
The SoH value after 800 cycles, at 25 °C and 1 C discharge rate.

SoH	$\Delta n = 0$	$\Delta n = 1$	$\Delta n = 2$	$\Delta n = 3$	$\Delta n = 4$	$\Delta n = 5$
$\Delta m = 0$	0 70.02%	2 75.39%	4 79.14%	6 81.90%	8 84.02%	10 85.69%
$\Delta m = 1$	5 80.62%	8 84.02%	11 86.40%	14 88.17%	17 91.23%	20 92.14%
$\Delta m = 2$	10 85.69%	14 88.17%	18 91.55%	22 92.65%	26 93.49%	30 94.16%

4. Computational method

The mean SoH of all the cells can be given by Eq. (6), i.e. $\mu = \text{SoH}$ during the operation of the cells. As each cell will degrade differently, the standard deviation of the SoH distribution will increase with the cycle number. Fig. 6 depicts the cell's SoH distribution in the battery pack with respect to the charge/discharge cycle number, and the dotted line is described by Eq. (6).

Unfortunately, the dependence of σ on the temperature, cycle number and C-rate is not available. On the other hand, the SoH distribution must be normal distribution by virtue of the central limit theorem. Since SoH cannot be more than 1, this will mean that the standard deviation σ at the start will have to be zero (this is possible due to our definition of SoH in Eq. (2)). As SoH degrades, σ will start to increase, but the increase must be such that its 6σ is at 1, thus we have,

$$\sigma = \frac{1-\mu}{6} = \frac{1}{6} \left[i \left(\frac{1}{2} k_1 N^2 + k_2 N \right) + \frac{k_3}{Q_{\max}(\text{new})} i \right] \tag{15}$$

4.1. Reliability of the battery pack I

Sony 18650 with the capacity of 1.75 A h is used in this work, so that the data in [17] can be employed. For illustration, the

Table 7
The SoH value after 500 cycles, at 50 °C and 1 C discharge rate.

SoH	$\Delta n = 0$	$\Delta n = 1$	$\Delta n = 2$	$\Delta n = 3$	$\Delta n = 4$	$\Delta n = 5$
$\Delta m = 0$	0	2	4	6	8	10
	58.68%	68.34%	74.57%	78.86%	82.88%	85.15%
$\Delta m = 1$	5	8	11	14	17	20
	76.90%	82.88%	86.08%	88.32%	89.96%	91.21%
$\Delta m = 2$						
	85.15%	88.32%	90.41%	91.89%	92.98%	93.83%

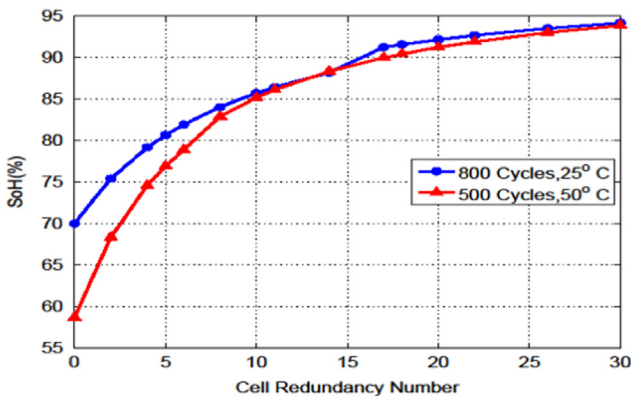


Fig. 9. The mean SoH of the battery pack w.r.t. the cell redundancy number. (For interpretation of the references to color in this figure legend, the reader is referred to the web version of this article.)

Table 8
The reliability by discharging 800 cycles, at 25 °C and 1 C discharge rate.

$R(G_s \geq 80\%)$	$\Delta n = 0$	$\Delta n = 1$	$\Delta n = 2$	$\Delta n = 3$	$\Delta n = 4$	$\Delta n = 5$
$\Delta m = 0$	0	2	4	6	8	10
	0	0.0002	0.0454	0.5600	0.9617	0.9993
$\Delta m = 1$	5	8	11	14	17	20
	0.6724	0.9983	1	1	1	1
$\Delta m = 2$	10	14	18	22	26	30
	1	1	1	1	1	1

structure of the battery pack I is assumed to be 2×5 parallel-series configuration. Using Eqs. (6) and (15), the probability density function of the cells' SoH is shown in Fig. 7, and Table 2 gives the probability of the cell's SoH levels at 0.5 C rate and 25 °C. Fig. 8 shows the similar probability density function, and Table 3 gives the probability for the cell's SoH levels at 0.5 C rate and 50 °C. As the safe operating temperature range for Li-ion battery operation is less than 60 °C as reported [28], only two temperatures, 25 °C and 50 °C with 10 °C allowance for self-generated heat during operation, are considered.

To calculate the reliability of the battery pack, let us set the failure threshold as $W = 80\%$, as it is a common practice for Li-ion battery pack in EV applications [35]. To illustrate the computation of reliability, let us consider the u -function of the cells (i, j) in battery pack I after 600 charge/discharge cycle number at 0.5 C rate and 25 °C as follows

$$u_{(i,j)} = 0.0012z^4 + 0.4798z^3 + 0.5173z^2 + 0.0017z^1 + 0z^0, \tag{16}$$

$\forall i = 1, 2; j = 1, 2, 3, 4, 5$

and thus

$$U(z) = 0z^4 + 0.2082z^3 + 0.7918z^2 + 0z^1 + 0z^0 \tag{17}$$

Using Eqs. (13) and (14), where $g_{(i,j)}$ is from Eq. (13), we have

$$R(G_s \geq 80\%) = 0 + 0.2082 = 0.2082 \tag{18}$$

Similar calculations can be performed for different cycle numbers, temperature and C-rate, and the reliability of the battery pack I are shown in Tables 4 and 5 at 25 °C and 50 °C, respectively.

4.2. Reliability of the battery pack II

To investigate the relationship between the battery pack reliability and the active redundant cell number and configuration, we consider two operating conditions for battery pack II. One is charged/discharged for 800 cycles at 25 °C, and another one is charged/discharged 500 cycles at 50 °C. In both conditions, the discharge rate is 1 C in every parallel branch. The reason of choosing the two operating conditions is that their reliabilities could be improved significantly with active cells redundancy.

We first calculate the cells' SoH of the battery pack according to Eq. (6) for additional cells with different configurations. For example, when $\Delta m = 1$ and $\Delta n = 1$, the mean SoH value after charging/discharging for 800 cycles, at 25 °C and 1 C discharge rate can be calculated as follows,

$$\begin{aligned} \text{SoH} = 1 - & \left[\frac{1}{2} \times 8.5 \times 10^{-8} \times \left(\frac{2 \times 5 \times 800}{(2+1) \times (5+1)} \right)^2 + 2.5 \times 10^{-4} \right. \\ & \left. \times \frac{2 \times 5 \times 800}{(2+1) \times (5+1)} \right] \\ & - 7.26 \times 10^{-2} \times \frac{2 \times 5 \times 1.75}{1.75 \times (2+1)(5+1)} = 0.8402 \tag{19} \end{aligned}$$

Table 9
The reliability by discharging 500 cycles, at 50 °C and 1 C discharge rate.

$R(G_s \geq 80\%)$	$\Delta n = 0$	$\Delta n = 1$	$\Delta n = 2$	$\Delta n = 3$	$\Delta n = 4$	$\Delta n = 5$
$\Delta m = 0$	0	2	4	6	8	10
$\Delta m = 1$	0	0	0	0.0185	0.8008	0.9965
$\Delta m = 2$	5	8	11	14	17	20
	0.0336	0.9774	1	1	1	1
	10	14	18	22	26	30
	1	1	1	1	1	1

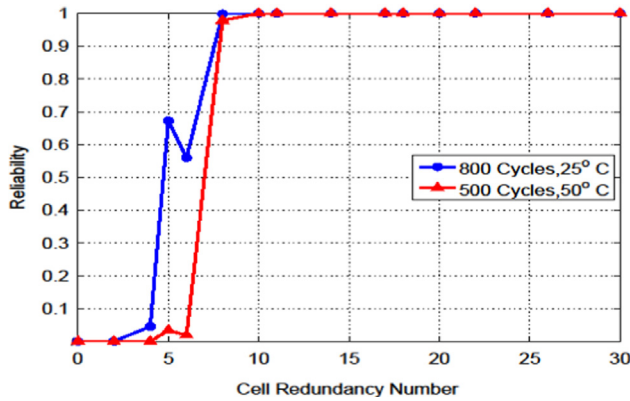


Fig. 10. The reliability with respect to the cell redundancy number.

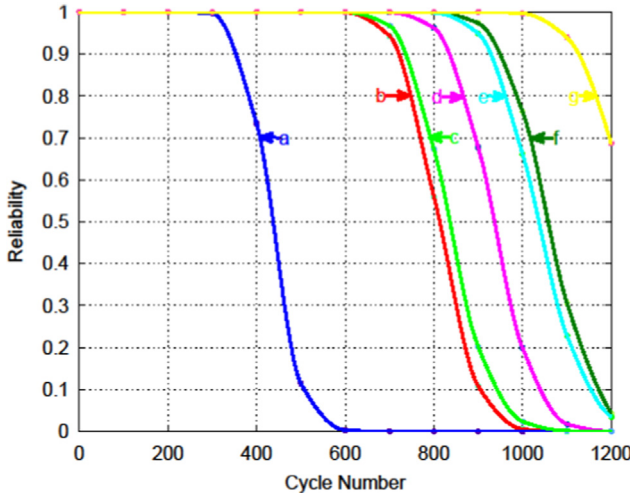


Fig. 11. The reliability of different configurations at 25 °C. (a) 2 × 5 configuration; (b) 2 × 8 configuration; (c) 3 × 5 configuration; (d) 2 × 9 configuration; (e) 3 × 6 configuration; (f) 2 × 10 configuration; (g) 4 × 5 configuration.

Similar calculations can be done for different Δm and Δn as shown in Tables 6 and 7. The percentage represents the SoH of each cell in the pack, and the integer above the percentage is the number of redundant cells. For example, for the case of $\Delta m = 1$, $\Delta n = 1$, “8” means that eight cells are added to the battery pack, and the configuration becomes 3 × 6 parallel-series.

From Tables 6 and 7, we can see that increasing the cells in the battery pack can improve the mean SoH of each cell in the battery pack regardless of the configuration. For example, considering the case of $\Delta m = 0$, $\Delta n = 4$, the SoH value is equal to the case of $\Delta m = 1$, $\Delta n = 1$, as the total number of the added cells in both configurations is 8. Therefore, we can conclude that when the number of the added cells is the same, the SoH of the battery pack will remain the same. We use red colour to show the SoH at the same redundant cell number. Fig. 9 shows the relationship between the cell mean SoH and the cell redundancy number.

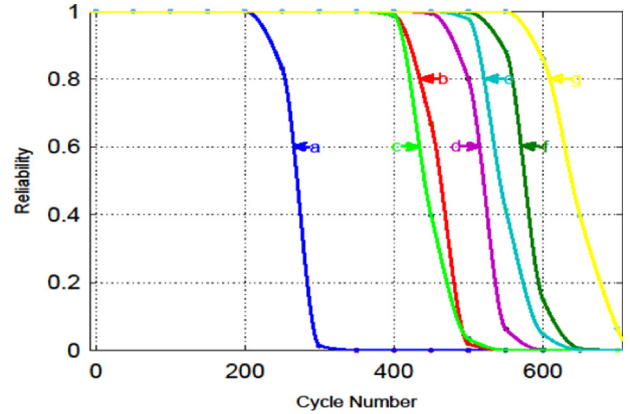


Fig. 12. The reliability of different configurations at 50 °C. (a) 2 × 5 configuration; (b) 2 × 8 configuration; (c) 3 × 5 configuration; (d) 2 × 9 configuration; (e) 3 × 6 configuration; (f) 2 × 10 configuration; (g) 4 × 5 configuration.

The reliability of the battery pack at the two different operating conditions is given in Tables 8 and 9, which are computed similarly as in the case of battery pack I. From Tables 8 and 9, we can see that the reliability of the battery pack can be improved by using cell redundancy as expected. We can also see that the amount of improvement in reliability is higher if we increase the parallel branch for a given number of redundant cells. For example, at 25 °C, the reliability by adding 8 cells in series configuration (i.e. 2 × 9) is 0.9617, while the reliability by adding 8 cells in parallel-series configuration (i.e. 3 × 6) is 0.9983. We also find that the reliability can be improved significantly by adding just 1 new parallel and 1 new series branches, and total number of added cell is only 8.

As adding more cells to the battery pack increases the cost of the battery pack, tradeoff between the additional cell number and the reliability must be considered for battery manufacturers. Fig. 10 shows the reliability improvement with respect to the cell redundancy number, and higher reliability values are chosen when the number of redundant cells is the same. For example, we choose 0.9983 as the reliability value for 8 redundant cells.

From Fig. 10, for 2 × 5 battery pack, it is very clear that adding 8 cells can obviously improve the reliability, from 0 to 0.9983 at 25 °C, and 0 to 0.9774 at 50 °C. However, we can also see in Fig. 10 that when the added cell number is 6, the reliability of the battery pack is lower than adding 5 cells due to the different configurations. The same issues could also be found in Fig. 11, which shows the reliability with respect to the cycle number for different configurations.

In Figs. 11 and 12, we can see that for the same charge/discharge cycle number, using cells redundancy could improve the reliability, but the configuration also has an effect on the reliability. For example, in Fig. 11, 2 × 10 configuration and 4 × 5 configuration have the same 10 redundant cells, but the 4 × 5 configuration has higher reliability. 3 × 5 configuration has smaller redundant cells than 2 × 8 configuration, but its reliability is higher.

We can also find the battery pack configuration with minimum cells for a desired reliability at a given cycle number from Figs. 11

and 12. For example, when we need to design a battery pack, if the battery pack is to be reliable ($R \geq 80\%$) after being charged/discharged 800 times, we can select 3×6 configuration, which demands a minimum cost.

Therefore, during the design of high reliability Li-ion battery pack, we should consider both the configuration and the cell redundancy number, as the relationship between the reliability, the cell number and the configuration of the battery pack is non-trivial.

5. Experimental challenges

To verify our proposed design concept, a small scale battery pack will be constructed, and the test experiments will be done. However, there are still some practical challenges in the experiments, so the experiment results cannot be shown in the paper now. First, the experiments will take a long time. For example, if we test some Li-ion battery packs (with 18650 cells) in safety operation range, it will take at least a few months to degrade the cells to its 80% capacity. Second, the experimental verification of the design concept proposed in the paper requires a lot of cells. It will take about 10 thousand dollars. Third, there are also some problems in the integration of the cells into the battery pack. The construction of the battery packs requires a thermal management system and a battery management system. The reliability of the battery pack is related to the temperature, SoC and SoH of the batteries, charging/discharging rate, depth of discharge and so on. So, according to these challenges, experimental verification of the design concept is a huge project, and industrial collaboration will be needed.

6. Conclusions

In this work, a concept for design-in reliability for Li-ion battery pack in EVs applications using cells redundancy is introduced, and the analysis is based on the SoH of the cells in the battery pack. We calculate the reliability of the battery packs with different configurations using UGF technique. Comparing the reliability of two battery packs at different temperatures, we conclude that the reliability could be improved by adding redundant cells as expected, and the configuration of the redundant cells has significant effect on its reliability. The proposed design concept provides a way to select the best redundant cells configuration for good pack reliability, while considering the total cost through the optimal number of the redundant cells.

While the proposed design concept is promising, there remain a few open issues such as its experimental validation which is also discussed, and reliability of thermal management and cell-to-cell interconnects in the battery packs, which are yet to be studied. The latter are assumed to be perfect in this work.

Acknowledgements

This work was financially supported by the Singapore National Research Foundation under its Campus for Research Excellence And Technological Enterprise (CREATE) programme.

Appendix A

A.1. Derivation of Eq. (6)

$$\begin{aligned} \text{SoH} &= \frac{Q_{\max}(\text{aged})}{Q_{\max}(\text{new})} = \frac{Q_{\max}(\text{new}) - Q_{\max}(\text{fade})}{Q_{\max}(\text{new})} \\ &= 1 - \frac{Q_{\text{lost}}(T, N) + Q_{\text{lost}}(i)}{Q_{\max}(\text{new})} \end{aligned}$$

$$\begin{aligned} &= 1 - \frac{Q_{\max}(\text{new}) \left(\frac{1}{2} k_1 N^2 + k_2 N \right)}{Q_{\max}(\text{new})} - \frac{k_3 i}{Q_{\max}(\text{new})} \\ &= 1 - \left(\frac{1}{2} k_1 N^2 + k_2 N \right) - \frac{k_3 i}{Q_{\max}(\text{new})} \end{aligned}$$

A.2. Central limit theorem (CLT)

Central limit theorem (CLT) states that, given certain conditions, the arithmetic mean of a sufficiently large number of iterates of independent random variables, each with a well-defined expected value and well-defined variance, will be approximately normally distributed. That is, suppose that a sample is obtained containing a large number of observations, each observation being randomly generated in a way that does not depend on the values of the other observations, and that the arithmetic average of the observed values is computed. If this procedure is performed many times, the central limit theorem says that the computed values of the average will be distributed according to the normal distribution.

References

- [1] Markolf R, Ohms D, Muller G, Chr Schulz, Harmel J, Wiesener K. Investigations into a battery management for high power nickel metal hydride batteries. *J Power Sources* 2006;154(2):902–5.
- [2] Chan CC, Chau KT. *Modern electric vehicle technology*. New York: Oxford University, Press Inc.; 2001.
- [3] Manenti A, Abba A, Merati A, Geraci A, Savaresi S. A new cell balancing architecture for li-ion battery packs based on cell redundancy. In: Proceedings of the 18th IFAC world congress, Milano, Italy, August 28–September 2; 2011, p. 12150–12155.
- [4] Nelson P, Dees D, Amine K, Henriksen G. Modeling thermal management of lithium-ion PNGV batteries. *J Power Sources* 2002;110(2):349–56.
- [5] Mills A, Al-Hallaj S. Simulation of passive thermal management system for lithium-ion battery packs. *J Power Sources* 2005;141(2):307–15.
- [6] Al-Hallaj S, Maleki H, Hong JS, Selman JR. Thermal modelling and design considerations of lithium-ion batteries. *J Power Sources* 1999;83(1-2):1–8.
- [7] Sato N. Thermal behaviour analysis of lithium-ion batteries for electric and hybrid vehicle. *J Power Sources* 2001;99(1-2):70–7.
- [8] Lee WC, Drury D, Mellor P. An integrated design of active balancing and redundancy at module level for electric vehicle batteries. In: 2012 IEEE transportation electrification conference and expo (ITEC); 2012. p. 1–6.
- [9] Jin FJ, Shin KG. Pack sizing and reconfiguration for management of large-scale batteries. In: Proceedings of the 2012 IEEE/ACM third international conference on cyber-physical systems (ICCPS 2012); 2012. p. 138–147.
- [10] Manenti A, Abba A, Merati A, Savaresi SM, Geraci A. A new BMS architecture based on cell redundancy. *IEEE Trans Ind Electron* 2011;58(9):4314–22.
- [11] Jofmeister J, Bush J, Vounout S. Prognostic health management (PHM) solutions for battery packs used in critical applications. In: The prognostics and health management solutions conference (MFPT2012); 2012. p. 1–15.
- [12] Wang ZP, Liu P, Chen W. Study of lifetime and reliability for power battery pack based on single battery failure. *High Technol Lett* 2010;16(1):18–22.
- [13] Plett GL. Recursive approximate weighted total least square estimation of battery cell total capacity. *J Power Sources* 2011;196(4):2319–31.
- [14] Spotnitz R. Simulation of capacity fade in lithium-ion batteries. *J Power Sources* 2003;113(1):72–80.
- [15] Stamps AT, Holland CE, White RE, Gatzke EP. Analysis of capacity fade in a lithium-ion battery. *J Power Sources* 2005;150:229–39.
- [16] Zhang Y, Wang C, Tang X. Cycling degradation of an automotive LiFePO4 lithium-ion battery. *J Power Sources* 2011;196(3):1513–20.
- [17] Ramadass P, Haran B, White R, Popov BN. Mathematical modeling of the capacity fade of li-ion cells. *J Power Sources* 2003;123(2):230–40.
- [18] Tippmann S, Walper D, Balboa L, Spier B, Bessler WG. Low-temperature charging of lithium-ion cells Part I: Electrochemical modelling and experimental investigation of degradation behaviour. *J Power Sources* 2014;252:305–16.
- [19] Han S, Han S, Aki H. A practical battery wear model for electric vehicle charging applications. *Appl Energy* 2014;113:1100–8.
- [20] Lisnianski A, Levitin G. *Multi-state system reliability: assessment, optimization and applications*. World Scientific; 2003.
- [21] Levitin G, Lisnianski A, Ben-Haim H, Elmakis D. Redundancy optimization for series-parallel multi-state system. *IEEE Trans Reliab* 1998;47(2):165–72.
- [22] Ouzineb M, Nourelfath M, Gendreau M. Tabu search for the redundancy allocation problem of homogenous series-parallel multi-state systems. *Reliab Eng Syst Saf* 2008;93(8):1257–72.
- [23] Tan CM, Raghavan N. A framework to practical predictive maintenance modeling for multi-state systems. *Reliab Eng Syst Saf* 2008;93(8):1138–50.

- [24] Tan CM, Raghavan N. Imperfect predictive maintenance model for multi-state systems with multiple failure modes and element failure dependency, In: Prognostics and system health management conference; 2010. p. 1–12.
- [25] Li CY, Chen X, Yi XS. Reliability analysis of primary battery packs based on the universal generating function method. *Proc Inst Mech Eng, Part O: J Risk Reliab* 2009;223:251–7.
- [26] Song BM, Han B, Lee JH. Optimum design domain of LED-based solid state lighting considering cost, energy consumption and reliability. *Microelectron Reliab* 2013;53(3):435–42.
- [27] Shan S, Wang GG. Reliable design space and complete single-loop reliability based design optimization. *Reliab Eng Syst Saf* 2008;93(8):1218–30.
- [28] Karadeniz H, Togan V, Vrouwenvelder T. An integrated reliability-based design optimization of offshore towers. *Reliab Eng Syst Saf* 2009;94(10):1510–6.
- [29] Ardakan MA, Hamadani A. Reliability optimization of series-parallel systems with mixed redundancy strategy in subsystems. *Reliab Eng Syst Saf* 2014;130:132–9.
- [30] Zhang CW, Zhang TL, Chen N, Jin TD. Reliability modeling and analysis for a novel design of modular converter system of wind turbines. *Reliab Eng Syst Saf* 2013;111:86–94.
- [31] Li YF, Zio E. A multi-state model for the reliability assessment of a distributed generation system via universal generating function. *Reliab Eng Syst Saf* 2012;106:28–36.
- [32] Tian ZG, Levitin G, Zuo MJ. A joint reliability-redundancy optimization approach for multi-state series-parallel systems. *Reliab Eng Syst Saf* 2009;94:1568–76.
- [33] Ng KS, Moo CS, Chen YP, Hsieh YC. Enhanced coulomb counting method for estimating state-of-charge and state-of-health of lithium-ion battery. *Appl Energy* 2009;86(9):1506–11.
- [34] Shahriari M, Farrokhi M. Online state-of-health estimation of VRLA batteries using state of charge. *IEEE Trans Ind Electron* 2013;60(1):191–202.
- [35] Electropaedia, Battery reliability and how to improve it, (<http://www.mpo-weruk.com/reliability.htm>), Oct. 2013.